FACILE SYNTHESIS OF CuO NANOPARTICLES BY HYDROTHERMAL METHOD AND THEIR APPLICATION ON ANTIBACTERIAL ACTIVITY

V. Maria Vinosel, A. Persis Amaliya, S. Blessi, S. Pauline*

Department of Physics, Loyola College, University of Madras, Chennai – 34, India
Corresponding author: paulantovero@yahoo.co.in

---***---

Abstract - *A versatile and surfactant free hydrothermal method was adopted to synthesize CuO nanoparticles. Using hydrothermal method CuO nanoparticles can be synthesized without organic solvents, expensive raw materials and complicated equipments. CuO nanoparticles were characterized by X-ray diffraction analysis (XRD), High resolution scanning electron microscopy (HRSEM), Energy dispersive X-ray analysis (EDAX), Fourier transform infrared (FTIR) and UV- visible spectroscopy. Structural analysis reveals that CuO nanoparticles have monoclinic structure with single crystalline phase. High resolution scanning electron microscopy exhibits rod like CuO nanostructures. Fourier Transform Infrared Spectroscopy spectra showed the vibrational bands of Cu-O metal oxygen bonds. Absorption spectra of CuO nanoparticles show broad absorption bands and band gap energy were determined. Antibacterial behaviors of CuO nanoparticles were also examined.*

Key Words: Copper Oxide, Nanorod, Monoclinic, Energy gap, Antibacterial

1. INTRODUCTION

CuO is a p-type semiconductor with a narrow band gap of 1.2eV is one of the most intensively studied metal oxide because of its potential applications in catalysis, solar cells, magnetic storage media, semiconductors, field transistors, gas sensors, batteries etc [1-3]. The surface morphology, size, shape and crystal structure of nanomaterials are important parameters that influence their chemical, optical and electrical properties [4]. Many methods have been developed for the preparation of CuO nanostructures including hydrothermal [5], thermal oxidation [6], electrochemical [7], solvothermal [8], simple hydrolysis [9], Microwave assisted and sol-gel [10] methods. Xiao et al. [11] synthesized CuO nanorods by using hydrothermal route in presence of sodium citrate. Liu and Bando et al. [12] synthesized nanodendrite and nanoshuttle like CuO nanostructures under surfactant assisted condition by hydrothermal route. However, hydrothermal solution phase synthesis, which has advantages such as low temperature, versatile synthetic process, great potential for scaling up, low-energy requirements, safe and environmentally benign synthetic conditions [13].

In this work, hydrothermal method was employed to synthesize CuO nanorod. The structure, morphology, elemental composition and optical properties of the as-prepared sample were characterized by XRD, HRSEM, EDX and UV-Vis. The antibacterial activity was also investigated.

2. EXPERIMENTAL

All the reagents used in the experiment were of analytical grade purity. CuO nanoparticles were prepared by hydrothermal method with Sodium hydroxide (NaOH) as precipitating agent. Copper precursor solution was prepared in a beaker by addition of 0.2M $CuCl_2.2H_2O$ and 0.4M of sodium hydroxide dissolved in 40ml of double distilled water. The aqueous solution of NaOH was added dropwise into the above solution under constant stirring. The pH value of the solution was maintained to be 10. The resultant solution was transferred to the stainless steel autoclave and hydrothermal synthesis was carried out for about 150°C for 12h. The obtained black precipitate was washed several times with deionized water and acetone to remove impurities. The final product is dried at 75°C for 6h.

3. ANTIBACTERIAL PERFORMANCE

30 mg of the CuO nanoparticles was suspended in 3.0 ml of Milli Q water to get a stock suspension of 10 mg/mL. From this stock suspension six different working suspensions of the concentrations 100, 200,300, 400, 500 and 600 µg were prepared with sterile deionized water in sterile test tubes. Using sterile cotton swab, the subculture of Staphylococcus aureus was made as a suspension in sterile Tryptone Soya broth. Using sterile micro tip7shallow wells were punched in the culture media with a gap of 1 cm between each well. The wells were marked at the base of the plate as 1,2,3,4,5,6 and control. With sterile micro tip 100 µL of each one of the 6 working CuO nanoparticle suspension was added to the duly marked wells. The bacterium was also exposed to an antibiotic disc containing 5µg of Ciprofloxacin, as an antibiotic control. The culture plate was incubated in the bacteriological incubator [Equitron] at 37°C for 24 h. After the incubation period the plate was examined for zone of inhibition.

4. RESULTS AND DISCUSSION

4.1 X-ray diffraction analysis

The crystal structure and purity of the synthesized CuO nanoparticles were determined by powder XRD. Fig.1

depicts the xrd pattern of CuO nanoparticles. The prominent diffraction peaks at 2θ values 32.5°, 35.5°, 38.9°, 48.7°, 53.5°, 55.2°, 58.5°are associated with [110], [$\bar{1}$11], [200], [$\bar{2}$02], [020], [021], [202] planes respectively. The evolved diffraction peaks could be indexed to a monoclinic phase of CuO with lattice parameters a= 4.683 Å, b= 3.421 Å, c= 5.129 Å and corresponds to the JCPDS file no 80-1268. The peak intensities and width of the spectrum indicates the presence of nanoscale crystallites. The absence peaks corresponding to byproducts such as $Cu(OH)_2$ or Cu_2O indicate the phase purity of CuO nanoparticles. The crystallite size is calculated using Debye Scherrer equation

$$d = \frac{0.9\,\lambda}{\beta\cos\theta}$$

Where d is the average crystallite size (nm), K is the grain shape factor (0.9), λ is the X-ray wavelength (nm), β is the line broadening at half the maximum intensity in radians, and θ is the Bragg diffraction angle of the 2θ peak. The average crystallite size was estimated to be 25 nm.
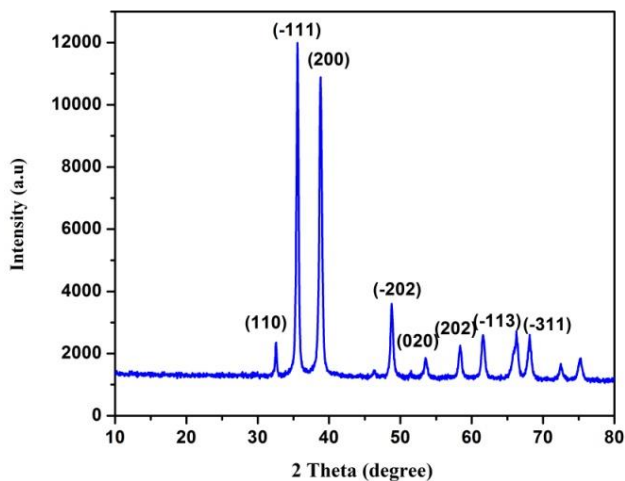

Figure1: XRD pattern of CuO nanoparticles

4.2 Scanning Electron Microscopy

The surface structure and elemental composition of copper oxide nanoparticles were probed using HRSEM and EDX. The morphology of CuO nanoparticles for different magnification is shown in Fig.2. CuO resembles nanorod like morphology with some agglomeration .The elemental analysis of the sample was performed by energy dispersive X-ray spectroscopy (EDX). The EDX spectrum of CuO nanoparticles in Fig.3 confirms the presence of Cu and O elements in the sample.
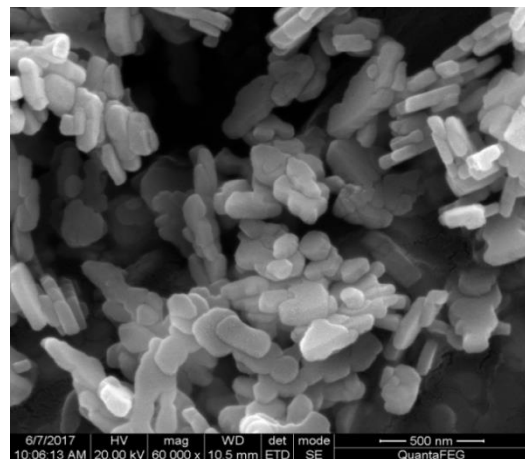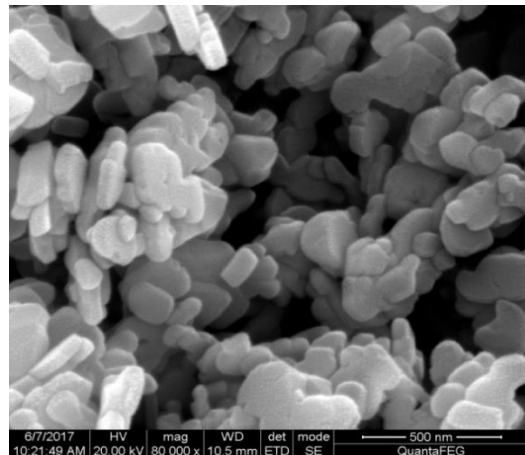

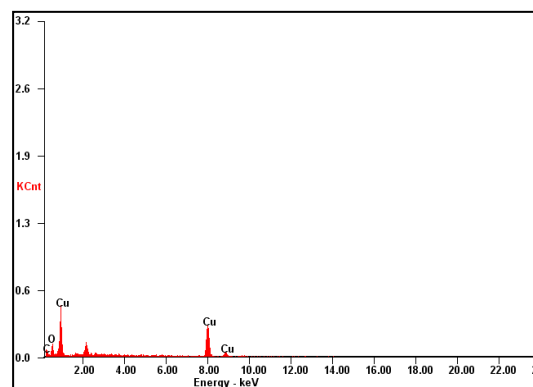**Figure2:** SEM micrograph of CuO nanoparticles

Figure 3: EDX analysis of CuO nanoparticles

4.3 FT-IR analysis

The FTIR transmission spectra of CuO nanoparticles are shown in fig 4. FTIR analysis was used to determine the functional groups of copper oxide nanoparticles. It can be observed apparently that the bands at 493 cm^{-1} and 613 cm^{-1} were assigned to be symmetric and asymmetric stretching modes of vibration metal oxygen bond. The broad absorption peak at 3426 cm^{-1} indicates the presence of

hydroxyl group representing the water as moisture in the sample. The FTIR spectra of the sample confirm the absence of any other residual organic compound. It is prominent that no infrared active modes from Cu_2O were detected, which is in good agreement with the XRD result.
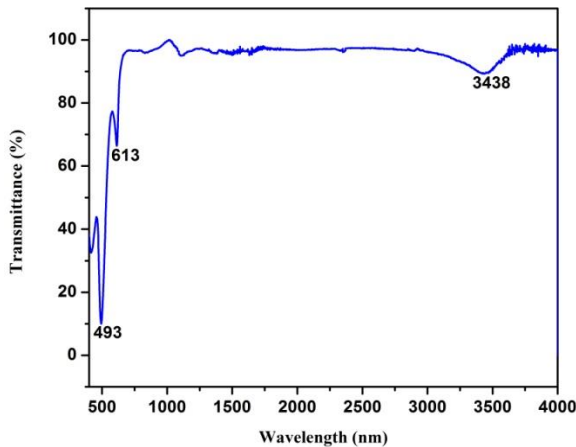

Figure 4: FTIR spectrum of CuO nanoparticles

4.4 UV-Visible spectra

UV-Visible absorption and band gap spectra for CuO nanoparticles are shown in fig 5. The spectrum shows the band edge-absorption peak which is found to be at 410 nm. In UV-Vis, high energy electromagnetic radiation in the wavelength range of 100-2000 nm is utilized to promote electrons to higher energy orbitals. The fundamental absorption, which corresponds to electron excitation from the valence band to the conduction band, can be used to determine the value of the optical band gap. The relationship between the absorption coefficient α and the incident photon energy $h\upsilon$ can be written as

$$(\alpha h\upsilon) = A (h\upsilon - E_g)^n$$

Where A is a constant and E_g the band gap in electron volt (eV) .Using equation the calculated value of the band gap energy for the synthesized CuO nanoparticle is 1.4 eV. The band gap increases with the decrease in the particle size. The direct energy band gap is calculated from the $(\alpha h\upsilon)^{1/n}$ Vs $h\upsilon$ plot.
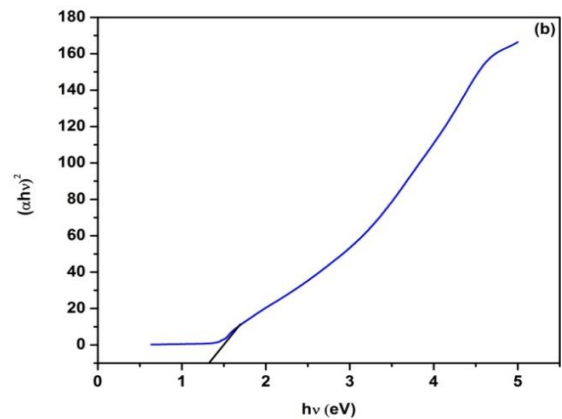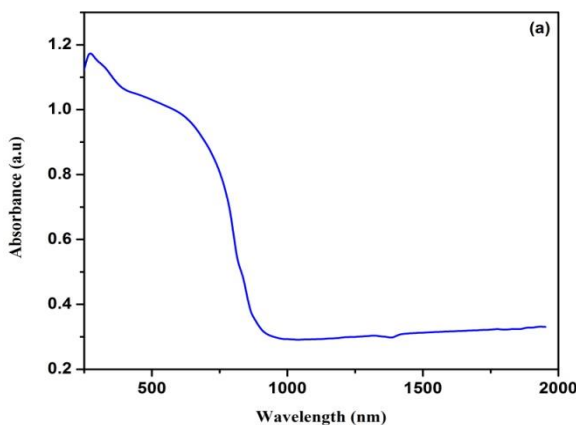

Figure 5: (a) UV-Vis absorption spectrum and (b) Tauc's plot

5. ANTIBACTERIAL ACTIVITY

The antibacterial activity of prepared CuO nanoparticles on the microorganism gram positive bacteria Staphylococcus aureus has been evaluated. Fig.6 shows a significant inhibition zone on the growth of bacteria with respect to the positive control for different concentrations of CuO nanoparticle. The possible mechanism of action is that the metal nanoparticles are carrying the positive charges and the microbes are having the negative charges which create the electromagnetic attraction between the nanoparticles and the microbes. When the attraction is made, the microbes get oxidized and die instantly. Generally, the nanomaterials release ions, which react with the thiol groups (–SH) of the proteins present on the bacterial cell surface which leads to cell lysis. The inhibition zone is found to increase with increase in the concentration of CuO nanoparticles. Nanoparticles tend to adsorb on the bacterial cell wall and undergo dehydrogenation due to respiration process which occurs at the cell membrane of bacteria. After reaction with nanoparticles, the bacteria had inactivated their enzymes, generating hydrogen peroxide that causes bacterial cell death.
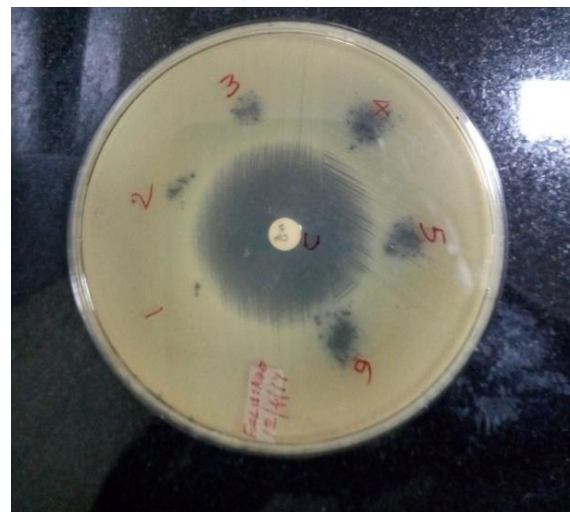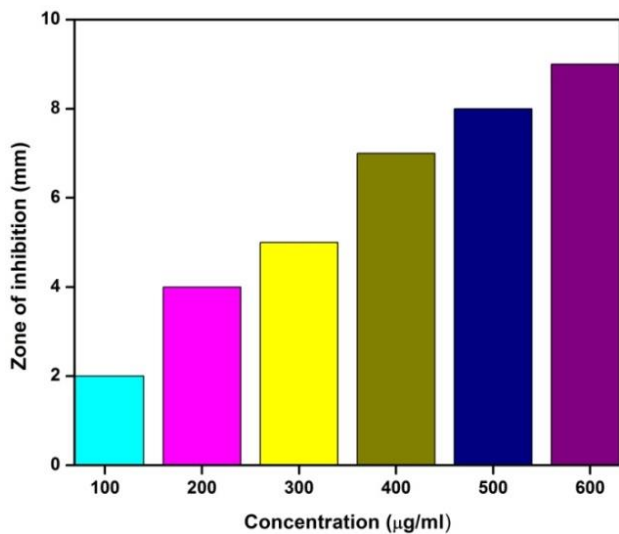
Figure 6: Zone of inhibition of CuO nanoparticles against Staphylococcus aureus

6. CONCLUSION

CuO nanoparticles were successfully synthesized by hydrothermal method. The formation of nanorod-like structure was authenticated by HRSEM analyses. Obtained values of MIC for S. aureus strains suggest that the prepared copper oxide nanoparticles shows excellent antibacterial activity and can be used as promising antibacterial agents in wide applications. The effect was dose dependent and was more pronounced against gram positive organism.

REFERENCES

1. C. Yang, X. Su, J. Wang, X. Cao, S. Wang, L. Zhang, Sens. Actuators B 185 (2013) 159-165.

2. T.X. Wang, S.H. Xu, F.X. Yang, Powder Technol. 228 (2012) 128-130.

3. K.M. Srestha, C.M. Sorensen, K.J. Klabunde, J. Phys. Chem. C 114 (2010) 14368-14376.

4. M.A. Dar, Y.S. Kim, W.B. Kim , J.M. Sohn , H.S. Shin , Applied Surface Science 254 (2008) 7477–7481.

5. D. Keyson, D.P. Volanti, L.S. Cavalcante, A.Z. Simões, J.A. Varela, E. Longo, Mater. Res. Bull. 43 (2008) 771–775.

6. J.T. Chen, F. Zhang, J.Wang, G.A. Zhang, B.B. Miao, X.Y. Fan, D. Yan, P.X. Yan, J. Alloys Compd. 454 (2008) 268–273.

7. G.-Q. Yuan, H.-F. Jiang, C. Lin, S.-J. Liao, J. Cryst. Growth 303 (2007) 400–406.

8. X.-L. Tang, L. Ren, L.-N. Sun, W.-G. Tian, M.-H. Cao, C.-W. Hu, Chem. Res. Chin.Univ. 22 (2006) 547–551.

9. Zhu, H. Bi, Y. Wang, X. Wang, X. Yang, L. Lu, Mater. Lett. 61 (2007) 5236–5238.

10. Y.-K. Su, C.-M. Shen, H.-T. Yang, H.-L. Li, H.-J. Gao, Met. Soc. China 17 (2007) 783–786.

11. H.M. Xiao, L.P. Zhu, X.M. Liu, S.Y. Fu, Solid State Commun. 141 (2007) 431.

12. Z. Liu, Y. Bando, Adv. Mater. 15 (2003) 303.

13. M.A. Dar, Q. Ahsanulhaq, Y.S. Kim c, J.M. Sohn, W.B. Kim, H.S. Shin, Applied Surface Science 255 (2009) 6279–6284.